Accepted: 29 May 2023

DOI: 10.1002/lsm.23695

BASIC SCIENCE ARTICLE

Deconvolution of the fluorescence spectra measured through a needle probe to assess the functional state of the liver

Ksenia Y. Kandurova MSc[1] | **Dmitry S. Sumin MD**[1,2] | **Andrian V. Mamoshin MD, PhD**[1,2] | **Elena V. Potapova PhD**[1]

[1]Research and Development Center of Biomedical Photonics, Orel State University, Orel, Russia

[2]Department of Interventional Radiology, Orel Regional Clinical Hospital, Orel, Russia

Correspondence

Ksenia Y. Kandurova, MSc, Research and Development Center of Biomedical Photonics, Orel State University, Orel 302026, Russia.
Email: kandkseniya@gmail.com

Abstract

Objectives: Currently, one of the most pressing issues for surgeons in the treatment of obstructive jaundice is the ability to assess the functional state of the liver and to detect and determine the degree of liver failure in a timely manner with simple and objective techniques. In this regard, the use of fluorescence spectroscopy method can be considered as one of the ways to improve the informativity of existing diagnostic algorithms in clinical practice and to introduce new diagnostic tools. Thus, the aim of the work was to study in vivo the functional state of liver parenchyma by the method of fluorescence spectroscopy implemented through a needle probe and assess the contribution of the main tissue fluorophores to reveal new diagnostic criteria.

Materials and Methods: We compared data from 20 patients diagnosed with obstructive jaundice and 11 patients without this syndrome. Measurements were performed using a fluorescence spectroscopy method at excitation wavelengths of 365 and 450 nm. Data were collected using a 1 mm fiber optic needle probe. The analysis was based on the comparison of the results of deconvolution with the combinations of Gaussian curves reflecting the contribution of the pure fluorophores in the liver tissues.

Results: The results showed a statistically significant increase in the contribution of curves reflecting NAD(P)H fluorescence, bilirubin, and flavins in the group of patients with obstructive jaundice. This and the calculated redox ratio values indicated that the energy metabolism of the hepatocytes may have shifted to glycolysis due to hypoxia. An increase in vitamin A fluorescence was also observed. It may also serve as a marker of liver damage, indicating impaired vitamin A mobilization from the liver due to cholestasis.

Conclusions: The results obtained reflect changes associated with shifts in the content of the main fluorophores characterizing hepatocyte dysfunction caused by accumulation of bilirubin and bile acids and after disturbance of oxygen utilization. The contributions of NAD(P)H, flavins, and bilirubin as well as vitamin A can be used for further studies as promising diagnostic and prognostic markers for the course of liver failure. Further work will include collecting fluorescence spectroscopy data in patients with different clinical effects of obstructive jaundice on postoperative clinical outcome after biliary decompression.

KEYWORDS

fluorescence spectroscopy, liver, liver failure, obstructive jaundice, optical biopsy

INTRODUCTION

Diagnostics and treatment of hepatopancreatoduodenal diseases complicated by biliary obstruction remains an urgent medical problem. In general, obstructive jaundice results from bile outflow disturbance through biliary tracts into duodenum. Obstructive jaundice may typically develop acutely as a result of biliary tract obstruction by gallstones in common bile duct, or develop gradually due to edema, stenosis, or tumor growth into intrahepatic and extrahepatic bile ducts. As the number of patients with obstructive jaundice of various etiologies increases every year this syndrome remains one of the common surgical problems and accompanying symptoms of hepatobiliary diseases with significant morbidity and mortality.[1]

Timely assessment of the liver state in jaundice and subsequent treatment is an important task since biliary obstruction causes hepatocyte dysfunction and impaired detoxification and synthesis functions of the liver. Resulting severe hemodynamic, metabolic, coagulation, and immune complications in the liver may lead to life-threatening functional and morphologic disorders in other vital organs.[2–4]

Despite the high level of modern methods for differential diagnosis of obstructive jaundice, follow-up definition and prognosis of the degree of liver failure to achieve better treatment results remains a difficult task. The primary goal in treating patients with biliary obstruction is to decompress the bile ducts as early as possible to interrupt the progression of complications, in particular the development of liver failure.[5] In recent years, a two-stage treatment tactic has been widely used for treating diseases accompanied by obstructive jaundice, which involves curing cholestasis by minimally invasive interventions followed by radical surgery after regression of bilirubinemia.[6] However, there are still discussions about the role, sequence of diagnostic and treatment procedures, methods of bile duct decompression, and their influence on the development of liver failure and prognosis of further condition of a patient in general.[6–8]

To choose the method of further therapy, to predict the course of the disease, and achieve the best results of treatment, it is important to have an understanding of the changes occurring in the liver parenchyma due to liver failure.[9] The intensity and rate of changes in the liver depend on the rate of biliary hypertension increase, microcirculation disorders, tissue hypoxia, presence of inflammation in ducts, and duration of pathological influence.[10] Contemporary diagnostics of liver failure is based on the data of experimental, biochemical, and instrumental studies, supplemented by clinical observations. The levels of total and direct bilirubin, alkaline phosphatase, liver enzymes alanine aminotransferase, aspartate aminotransferase, and lactate dehydrogenase are usually considered as markers of obstructive jaundice and liver failure.[11] Since obstructive jaundice causes severe hemodynamic, metabolic, coagulation, and immune changes not only in the liver, but also in the whole organism, current clinical practice uses not only values of certain clinical and biochemical parameters but also many prognostic scales and systems to assess the severity of hepatocellular dysfunction.[12] Commonly used criteria include Child-Pugh and MELD (Model for End-Stage Liver Disease) scales, serum albumin-bilirubin levels (ALBI scale), and the indocyanine green (ICG) clearance test. However, the mentioned tools for assessment of liver functional reserves give approximate indirect results. Thus, the relevance of finding additional objective criteria for timely assessment of the progression of liver failure and developing technologies to use in routine clinical practice remains significant.

One of the ways to improve the informativity of existing diagnostic algorithms in clinical practice and to introduce new diagnostic tools is the application of biophotonics methods. These methods continue to be developed to solve the problems in many fields of biology and medicine, including oncology and surgery.[13–20] The advantages of these methods are related to their good resolution, low cost of the procedure, higher productivity, and safety. Optical diagnostic methods demonstrated their possibilities for in vivo analysis of liver tissue saturation,[21,22] metabolic changes in a variety of liver diseases,[23–25] as well as for discriminating tumors from liver parenchyma,[21,25,26] assessing and characterizing damage to nonmalignant liver tissue.[27] Therefore, the development of scientific and instrumental bases to create methods for in vivo analysis of hepatic functional state is one of the promising trends.

A wide range of approaches to optical diagnostics in surgery are based on the fluorescence phenomenon. In particular, one of the most common and easier to implement method is fluorescence spectroscopy (FS). FS has a high sensitivity to metabolic changes in the tissue and remains a promising direction of tissue functional state assessment.[15,21] Assessment of the fluorescence intensity of certain fluorophores involved in biochemical reactions in cells (nicotinamides, flavins, fatty acids, bilirubin, porphyrin) makes it possible to assess the metabolic state of tissues. In turn, the content of fluorescing structural proteins (collagen, elastin) allows for the detection the presence of structural changes in tissues.[28] By evaluating the contributions of individual fluorophores, it is feasible to more accurately identify the causes and extent of changes in the functional state of tissues, associate them with pathological changes, and thus use them as criteria for in vivo diagnostics.[29–32] In addition, an important advantage of FS is the technical possibility of making measurements during minimally invasive procedures using small diameter probes.[25,33–35] We suppose that to solve the problem described, FS can be applied through a minimally invasive approach during primary antegrade decompression of the biliary tract

under ultrasound and X-ray control. The additional diagnostic information obtainable by using FS would allow surgeons to assess liver functional reserves before surgery, predict the course of the postoperative period, adjust therapy regimens in a timely manner, including indications for repeat surgery, include extracorporeal detoxification methods, or immediately initiate intensive therapy for progressive liver failure in particularly severe cases.

Thus, the aim of the work was to study in vivo the functional state of liver parenchyma in obstructive jaundice syndrome by the method of FS implemented through a needle probe and assess the contribution of the main tissue fluorophores to the composition of the registered fluorescence spectra to reveal new diagnostic criteria for future research.

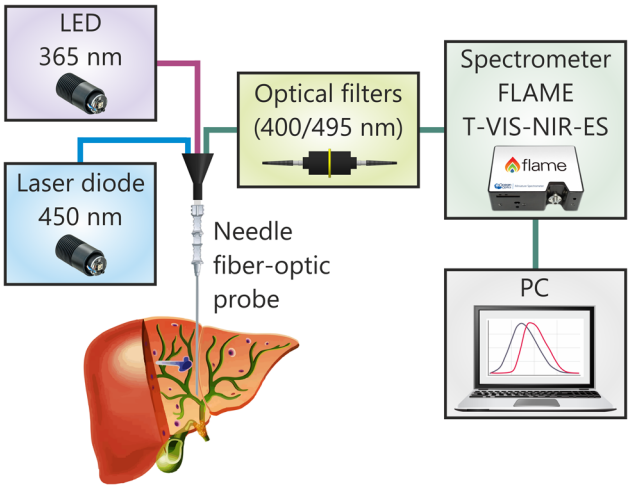

FIGURE 1 Schematic view of the setup for measuring fluorescence spectra of liver tissue.

MATERIALS AND METHODS

The study was conducted at the department of interventional radiology of Orel Regional Clinical Hospital (Orel, Russia). The study was approved by the Ethics committee of Orel State University (record of the meeting No. 14 of 24.01.2019) and carried out in accordance with the 2013 Declaration of Helsinki by the World Medical Association. All patients signed an informed consent indicating their voluntary participation in the study.

The study involved 20 patients with the diagnosis of obstructive jaundice. Among them 15 patients had malignant tumors as the cause of common bile duct obstruction, four patients had choledocholithiasis, one patient had cyst of pancreatic head. Exclusion criteria were patients with nonalcoholic fatty liver disease and alcoholic cirrhosis. Optical measurements were performed during the initial antegrade decompression of the biliary tract under ultrasound and X-ray control.

Since it is impossible to measure the liver tissue of healthy volunteers to create a control group without obstructive jaundice and other pathologies, we used the data obtained earlier in the studies described in more detail in the paper by Dremin et al.[21] Patients with malignant neoplasms of the liver who had optical measurements performed during a routine puncture biopsy procedure participated in this study. Fluorescence spectra were recorded along the path of the puncture needle and fiber optic probe in tissues unaffected by the malignant neoplasm. The comparison group included data of 11 patients who were not diagnosed with obstructive jaundice syndrome. Thus, it was possible to compare fluorescence spectra with and without this condition.

Measurements were performed using a FS channel of the specially designed optical biopsy setup (Figure 1). A 365 nm LED and a 450 nm laser diode were used as sources of monochromatic radiation. The radiation power of the sources did not exceed 0.2 mW at the tip of the needle probe to avoid significant photobleaching effects and not to cause damage to biological tissues.[36,37] The choice of the wavelengths was mainly aimed at exciting the fluorescence of nicotinamides and flavins as well as bilirubin and, to a lesser extent, a number of other fluorophores, the contribution of which was evaluated by further processing. Fluorescence spectra were recorded using a FLAME T-VIS-NIR-ES CCD spectrometer (Ocean Optics) in the 350–1000 nm range after attenuation of backscattered radiation from sources when passing through FGL400 and FGL495 filters (Thorlabs Inc.). Optical radiation was transmitted from the sources to the liver tissues and from the tissues to the spectrometer via nine 100 µm optical fibers around a one 200 µm optical fiber inside a specially designed fiber-optic probe with a diameter of 1 mm. The central fiber was used to connect to the spectrometer, and three 100 µm fibers (six in total) were used to connect to each radiation source. The diameter of the probe and the 20-degree bevel of the rigid end was designed to be compatible with standard 17.5 G Chiba-type biopsy needles.

The experimental design is described in Figure 2. Fluorescence spectra were analyzed using the OriginPro 2021 9.8 software (http://www.originlab.com, RRID: SCR_014212). During a single study, five fluorescence spectra at each wavelength were recorded at one to two points for each patient, then the data were averaged for the same point. Thus, 35 averaged spectra for 365 nm excitation and 26 spectra for 450 nm excitation were analyzed next. The comparison group had 11 spectra, each one was averaged over 10 measurements in a single point of liver tissue. The averaged fluorescence spectra were smoothed using the Savitzky–Golay filter to exclude noise, but without affecting the shape of the spectra. The smoothed spectra were normalized from 0 to 100. The next stage of processing included nonlinear

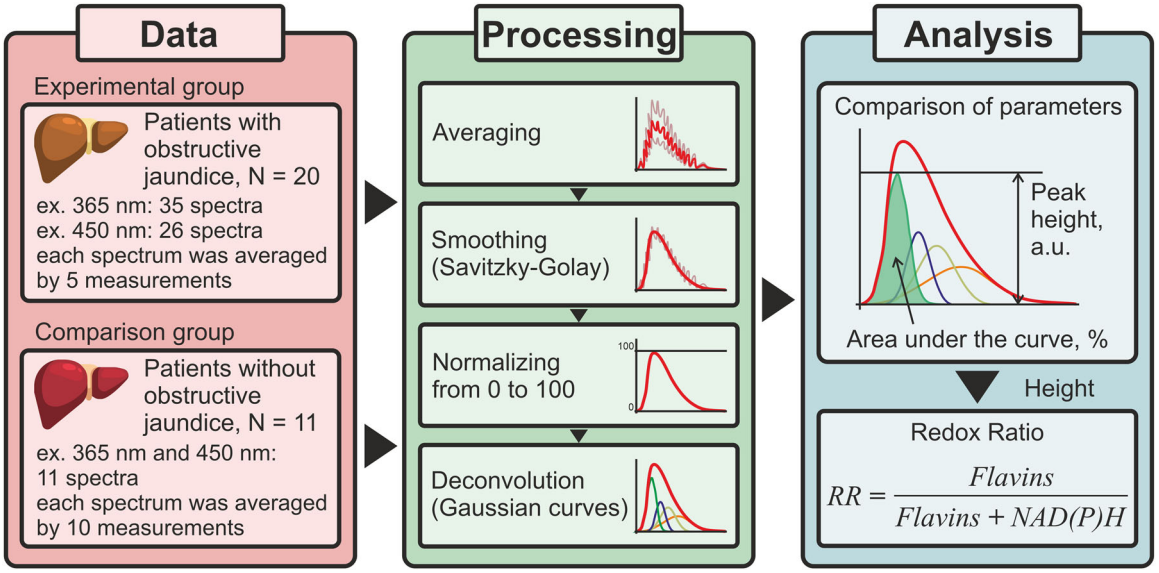

FIGURE 2 Schematic diagram of the experimental design.

curve-fitting procedure of deconvolution based on the Levenberg–Marquardt algorithm to calculate the linear combinations of Gaussian curves reflecting the contribution of pure fluorophores to the total signal obtained from liver tissue. The quantity of curves, their central wavelengths, and full widths at half maximum were initially selected from the literature findings on the fluorescence composition of the liver parenchyma, and then adjusted empirically to provide as best as possible fit for the measured spectra profiles.[28,30,31,38] The quality of the convergence of the curves was verified by the values of residuals and r^2 coefficient of determination.

Figure 3 shows examples of fluorescence spectra deconvolution into selected components. A total of 10 curves for fluorescence spectra excited by 365 nm (Figure 3A) and four curves for excited by 450 nm radiation (Figure 3B) were extracted to obtain information about the potential contribution of fluorophores to the emission spectra of liver parenchyma.

Curve 1 shows the effect of fluorescence of collagen and elastin which are fibrous proteins in the connective tissues.[39] Curve 2 is a reduced form of nicotinamide adenine dinucleotide and nicotinamide adenine dinucleotide phosphate (NADH and NADPH, commonly referred to together as NAD(P)H). NAD(P)H is involved in energy metabolism reactions in cell mitochondria, acting as one of the main electron donors in the Krebs cycle.[40,41] Curve 3 reflects the contribution of fluorescence of free fatty acids synthesized by the liver, and curve 4 represents the fluorescence of vitamin A indicating retinoid metabolism.[42] Assessment of input from these fluorophores is used less frequently, but the potential of these parameters as diagnostic criteria has been noted in the literature.[28]

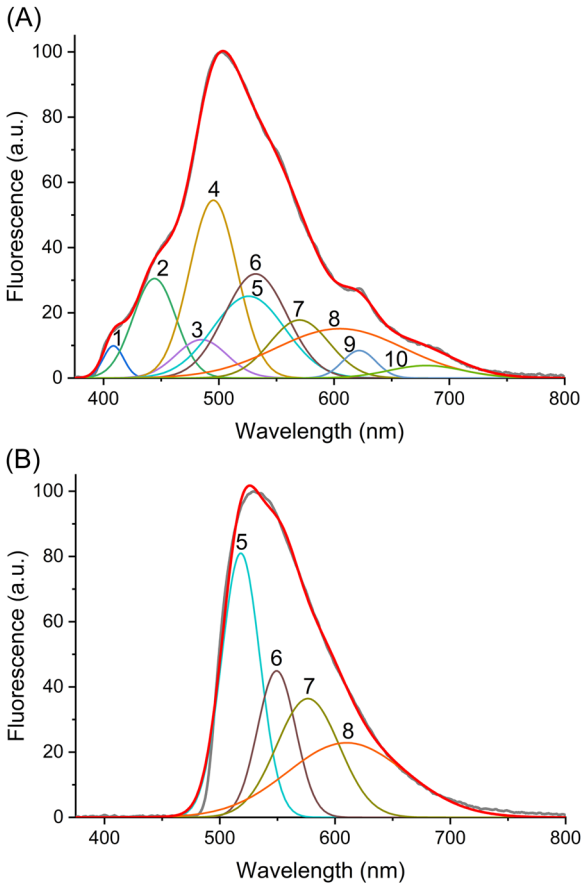

FIGURE 3 Examples of fluorescence spectra deconvolution in liver tissues for the excitation wavelengths of 365 nm (A) and 450 nm (B): 1, fibrous proteins (collagen and elastin); 2, NAD(P)H; 3, fatty acids; 4, vitamin A; 5, 7, bilirubin (two peaks at approx. 520 and 570 nm); 6, flavins; 8, lipofuscin; 9, protoporphyrin IX; 10, porphyrin derivatives.

Curves 5 and 7 represent two characteristic peaks found in the fluorescence spectra of bilirubin, a product of hemoglobin decay, which is converted from the water-soluble unconjugated form (indirect) to the conjugated (direct) one in hepatocytes and excreted with bile. Bilirubin is one of the pigments responsible for bile's typical color. Bilirubin fluorescence spectrum shows a major band around 520–530 nm and additional minor bands (taking into account the range of obtained data, the second band around 560–570 nm was chosen).[43] Curve 6 represents the fluorescence of flavins also involved in the energy metabolism reactions.[28] Curve 8 is located in the wide fluorescence range of lipofuscin pigment which is an indicator of oxidative stress and ageing.[44,45] Curves 9 and 10 belong to the characteristic fluorescence peaks of protoporphyrin IX and other porphyrin derivatives—the precursors to heme, and accordingly to hemoglobin.[46] Fluorophores from five to eight match those for both types of spectra, but the emission maxima and hence the central wavelengths of the Gaussian curves are shifted to the right (redshifted).

The analyzed parameters included peak heights, areas under Gaussian curves, and their relative contribution to the total areas of spectra curves. The statistical significance of the differences between the parameters was checked using the nonparametric Mann–Whitney *U* test due to the limited sample size and lack of confirmed normal distribution of the results in all compared samples.

RESULTS

Figure 4 shows the averaged normalized fluorescence spectra for both groups. Fluorescence spectra for 365 nm excitation showed no wavelength shift in the fluorescence maximum, but the group of patients with obstructive jaundice showed increased fluorescence at about 400–450 nm and decreased fluorescence at about 550–700 nm. The 450 nm spectra showed slight blue shift for the wavelength of maximum fluorescence value and a decrease in the range around 550–750 nm for group of patients with obstructive jaundice.

Table 1 shows the results of calculation of the selected parameters for all fluorophores in the 365 nm spectra. The highest height values were expectedly observed for the components characterizing the fluorophores with emission spectra closest to the maximum of the entire spectrum, in particular, vitamin A and flavins. Significant contribution of lipofuscin was also noticeable, but there were no statistically significant differences. The group of patients with obstructive jaundice showed statistically significant increase of curves height for NAD(P)H and vitamin A and decrease—for fatty acids. Protein and porphyrin curves also contributed little at the edges of the spectra, but it is worth noting that the profiles of some spectra displayed a small characteristic fluorescence increase from protoporphyrin IX around 625 nm.

The parameter of the area percentage under the particular Gaussian curves in the total spectrum area shows more statistically significant differences between the groups. The greatest contribution to the spectral area was due to the lipofuscin curve, which, as in the case of the peak height, exhibited a large scattering of area values. The high level of vitamin A fluorescence was also noticeable again. The proportion of the areas of bilirubin curves shows no statistically significant differences between the groups in contrast to the flavins, which undergo an increase in the area contribution in the same way as NAD(P)H, which may indicate the differences in energy metabolism.

The results of calculations for spectra excited by 450 nm are shown in Table 2. For both parameters, there was an increase in bilirubin and flavins contributions in the group of mechanical jaundice patients and a decrease in lipofuscin contributions. A twofold predominance of the main peak of bilirubin fluorescence relative to the

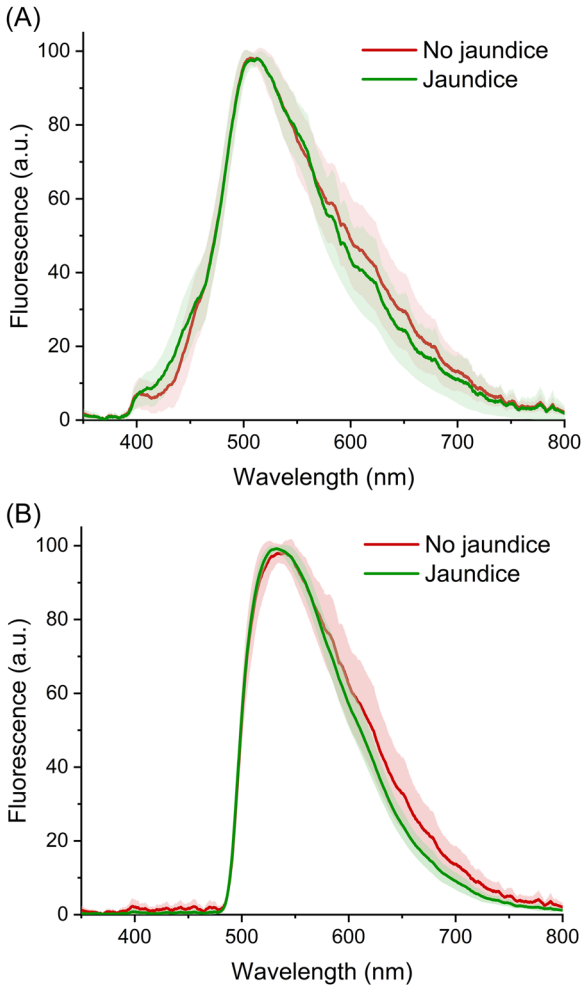

FIGURE 4 Averaged normalized (mean ± standard deviation) fluorescence spectra of liver tissues for the excitation wavelengths of 365 nm (A) and 450 nm (B).

TABLE 1 Results of calculation of Gaussian curves parameters in fluorescence spectra obtained under 365 nm excitation, median (25th and 75th percentiles).

Fluorophores	Peak height, a.u.		Area under the curve, %	
	No jaundice	Jaundice	No jaundice	Jaundice
1. Fibrous proteins[28,30,32,39]	5.1 (4.4–9.2)	7.9 (3.3–9.6)	0.8 (0.6–1.6)	1.2 (0.5–1.6)
(λ = 405 nm; FWHM = 21 nm)				
2. NAD(P)H[28–30,32,39]	8.5 (7.4–9.8)	17.3 (14.0–27.8)*	2.6 (2.5–3.1)	5.9 (4.5–10.3)*
(λ = 448 nm; FWHM = 44 nm)				
3. Fatty acids[28,30,47]	7.7 (0.0–14.0)	0.1 (0.0–3.4)*	3.0 (0.0–5.0)	0.3 (0.0–1.5)*
(λ = 482 nm; FWHM = 53 nm)				
4. Vitamin A[28,30]	43.0 (36.8–50.3)	50.9 (46.3–61.1)*	14.1 (13.7–18.0)	19.2 (16.0–24.6)*
(λ = 497 nm; FWHM = 49 nm)				
5. Bilirubin (1st peak)[28,30,43]	23.9 (23.3–27.9)	22.0 (19.0–24.7)	13.7 (11.9–15.2)	12.6 (9.7–14.2)
(λ = 522 nm; FWHM = 74 nm)				
6. Flavins[28–30,32]	30.2 (27.5–36.5)	34.6 (32.7–38.6)	14.4 (12.6–17.3)	17.5 (15.0–19.7)*
(λ = 530 nm; FWHM = 65 nm)				
7. Bilirubin (2nd peak)[28,30,43]	19.7 (16.7–20.6)	18.4 (17.0–20.2)	8.6 (8.3–9.6)	8.6 (7.8–9.5)
(λ = 569 nm; FWHM = 61 nm)				
8. Lipofuscin[28,30,32]	37.3 (26.3–44.0)	27.2 (18.5–33.4)	35.7 (27.1–39.5)	26.7 (19.8–31.6)*
(λ = 603 nm; FWHM = 131 nm)				
9. Protoporphyrin IX[28–30]	4.1 (3.1–7.4)	6.4 (5.0–7.7)	1.1(0.8–2.1)	1.8 (1.4–2.4)*
(λ = 618 nm; FWHM = 35 nm)				
10. Porphyrin derivatives[28–30]	6.9 (2.7–9.2)	4.0 (2.6–5.6)	3.8 (1.7–4.8)	2.5 (1.6–3.2)
(λ = 679 nm; FWHM = 76 nm)				

Abbreviations: λ, central wavelength; FWHM, full width at half maximum.
*Statistically significant differences for $p < 0.05$.

TABLE 2 Results of calculation of Gaussian curves parameters in fluorescence spectra obtained under 450 nm excitation, median (25th and 75th percentiles).

Fluorophores	Peak height, a.u.		Area under the curve, %	
	No jaundice	Jaundice	No jaundice	Jaundice
5. bilirubin[28,30,43] (1st peak)	74.0 (70.2–80.6)	79.0 (74.7–81.6)	22.3 (20.7–28.8)	27.2 (25.5–29.0)*
(λ = 518 nm; FWHM = 39 nm)				
6. Flavins[28–30,32]	39.7 (34.8–44.4)	46.0 (43.7–48.5)*	12.3 (10.3–15.6)	16.3 (15.3–17.4)*
(λ = 549 nm; FWHM = 39 nm)				
7. Bilirubin (2nd peak)[28,30,43]	32.4 (30.6–37.3)	37.4 (35.5–38.4)*	17.1 (15.0–19.7)	21.0 (19.4–22.2)*
(λ = 577 nm; FWHM = 63 nm)				
8. Lipofuscin[28,30,32]	49.9 (31.1–53.0)	31.1 (29.2–37.1)*	49.5 (35.2–53.6)	34.6 (32.6–39.8)*
(λ = 610 nm; FWHM = 123 nm)				

Abbreviations: λ, central wavelength; FWHM, full width at half maximum.
*Statistically significant differences for $p < 0.05$.

second curve of bilirubin and flavins was observed in terms of curve height. When comparing percentages of areas, the prevalence of bilirubin versus flavins contribution was noted.

The parameters of the curves in the range 450–600 nm underwent the most noticeable changes in the patients with obstructive jaundice. These changes were observed in fluorescence spectra for both emission sources, so we believe that it makes sense to consider them as potential markers of liver functional state in more detail. It is worth noting that the parameters of the curves representing the fluorescence of fatty acids took the values closest to zero more frequently, while there was also a large scatter for the group of patients without obstructive jaundice. In general, it is believed that the contribution of fatty acids to the total liver fluorescence is not very significant, and research toward taking it into account is not yet as widespread.[47,48]

Since the work is devoted to the search for new diagnostic tools for the evaluation of liver failure, we decided at this point to analyze more closely the energy metabolism and excretory function of the liver. Therefore, the results reflecting the levels of NAD(P)H, flavins, and bilirubin were considered separately. The contribution of vitamin A has also been evaluated separately as another important fluorophore that may hold promise as a possible marker for liver failure.

Based on the peak height fluorescence values of NAD(P)H at 365 nm excitation and flavins at 450 nm excitation, we additionally calculated the redox ratio, which is used to assess changes in cellular metabolism.[20,49,50] The redox ratio was calculated using one of the common approaches to its evaluation, according to the formula[28,51,52]:

$$RR = \frac{\text{Flavins}}{\text{Flavins} + \text{NAD(P)H}}. \quad (1)$$

Analysis of the parameters of the curves (Figure 5) showed a statistically significant predominance of NAD(P)H for both parameters (height and area) in the spectra excited by 365 nm radiation with the lowest value of p. Analysis of the curves obtained for spectra excited by 450 nm showed a statistically significant increase in the percentage of area of both bilirubin and flavin curves and less pronounced increase of this parameter for flavin curve and the second peak of bilirubin fluorescence.

The calculated redox ratios showed a statistically significant decrease of this parameter in the group of patients with obstructive jaundice (median 0.77, 25th and 75th percentiles 0.71–0.79) compared to patients without this syndrome (median 0.82, 25th and 75th percentiles 0.80–0.84).

DISCUSSION

The evaluation of biological tissues using FS data is a valuable source of information on changes in tissue structure and metabolic processes. Due to the fact that fluorescence spectra are composed of the contributions of a number of fluorophores fulfilling different metabolic and structural functions, the approach of decomposing fluorescence spectra into their main components has demonstrated ample opportunities for applications in various fields of medicine.[31,53,54] The possibilities of the technique we have chosen to obtain additional diagnostic information about the functional state of liver tissues using Gaussian curves have also been extensively demonstrated previously.[28,30,55] Fluorescence diagnostic methods are also increasingly being introduced with needle probes, so the application of spectral deconvolution to data obtained with such probes is a promising prospect. The results obtained allow us to conclude that it is possible to implement this methodology for the task in question.

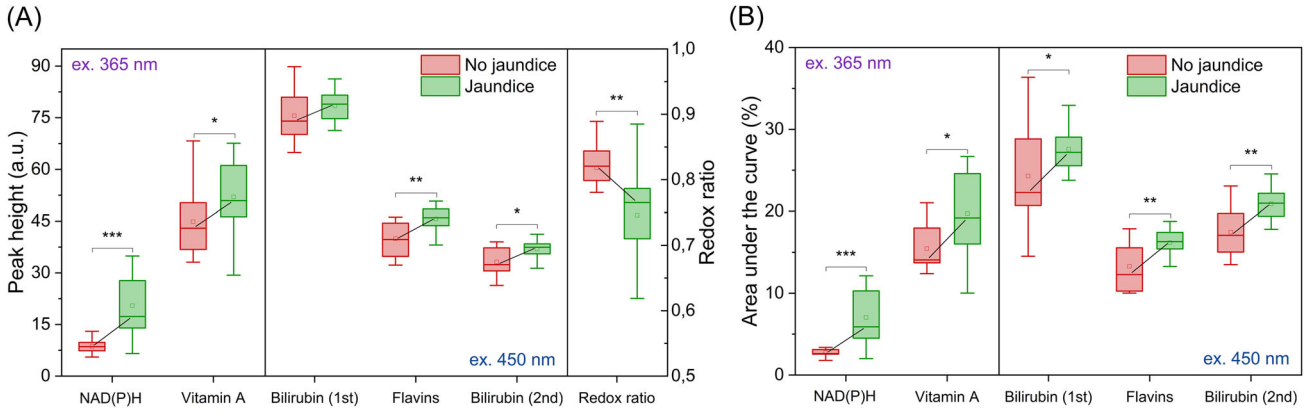

FIGURE 5 Comparison of the parameters of the Gaussian curves: peak height of the Gaussian curves and redox ratios (A), percentage of the area under the Gaussian curves of the fluorophores in the total area under the fluorescence spectrum curve obtained after nonlinear fitting (B). Median values are connected by the lines between groups. Statistically significant differences for: $*p < 0.05$, $**p < 0.01$, $***p < 0.001$.

In this series of experiments, we aimed at considering the influence of as many components of fluorescence spectra as possible (especially those excited by 365 nm light) for a more accurate fitting and evaluation to determine which fluorophores would be better suited for the diagnostic task described. Meanwhile, we made a number of assumptions when selecting the input parameters, based on technical capabilities and the lack of need for more detailed separation of individual curves within a group of fluorophores. In particular, we did not analyze the separate contribution of free and bound NAD(P)H fluorescence, as well as different types of free fatty acids.[28,56]

Next, the parameters of the curves of the fluorophores of interest for the assessment of the functional state of the liver—NAD(P)H, flavins, and bilirubin—were determined and analyzed in more detail. First of all, the increased contribution of bilirubin to the fluorescence spectra was an expected effect due to the fact that it is a direct consequence of the accumulation of high amounts of bilirubin, the outflow of which from the hepatic acini into the ducts is blocked. Developing biliary hypertension is one of the factors of disorders in blood supply to liver cells, resulting in damage to membranes of bile ducts and hepatocytes.

The results obtained for the remaining fluorophores, reflecting metabolic changes, are the above-mentioned consequence of the biliary obstruction and the shift in the bilirubin content. This leads to inhibition of oxidative phosphorylation and antioxidant protection of liver, reduction of bioenergetic processes in mitochondria of hepatocytes, inhibition of cytochrome oxidase and succinate dehydrogenase activity.[57,58] The prevalence of NAD(P)H may indicate impaired oxygen utilization leading to severe tissue hypoxia and following damage to hepatocytes and liver in general. Prolonged and progressive jaundice leads to impaired liver function, which eventually leads to liver failure, and hypoxia is considered to be one of the most common causes of this condition.[59] We assume that an electron donor in the cytosol, NADPH, may have influenced the NAD(P)H curve, but to a lesser extent than NADH. NADH and NADPH have indistinguishable fluorescence spectra but play different roles in cells. NADH is primarily involved in energy metabolism reactions, while NADPH is involved in anabolic reactions, including those related to antioxidant defense.[60] Since one of the factors of oxidative stress in various liver diseases is the activation of NADPH oxidase,[61,62] we hypothesize that most of the increase in NADH levels we observe is due to hypoxia rather than NADPH. However, a more accurate separation of the fluorescence of these cofactors by the FS method seems to be difficult.

Hepatocyte metabolic disturbances due to hypoxia were also indicated by the calculated redox ratios in liver tissue of patients with and without obstructive jaundice. Changes in the rate of cellular metabolism are reflected by the redox ratio.[49] According to the method we used to calculate the redox ratio, its decrease can be interpreted as an increase in the metabolic activity of the cell or the predominance of glycolysis over oxidative phosphorylation due to hypoxia. During oxidative phosphorylation, NAD(P)H loses an electron and is converted to NAD(P)+, which does not fluoresce. In contrast, NAD(P)H accumulates during glycolysis. In the case of flavins, the fluorescent coenzyme flavin adenine dinucleotide (FAD) is formed predominantly by oxidative phosphorylation from the nonfluorescent form $FADH_2$. When hypoxia occurs, the glycolytic pathway becomes more pronounced in the cell, leading to an increase in NAD(P)H content and consequently an increase in its fluorescence contribution, which decreases the value of the redox ratio. It is the decrease in this ratio that has been found in the liver tissue of patients with obstructive jaundice.[51,52,63]

In addition to the fluorophores discussed as possible markers of liver function, we found statistically significant differences in the contribution of vitamin A fluorescence. According to the literature, the liver is normally characterized by a remarkable content of vitamin A, which, among other factors, was considered as an additional factor affecting the possibility of detecting NAD(P)H fluorescence.[64,65] However, since the liver is the site of vitamin A storage in the human body, the impairment of normal liver function, including that due to obstructive jaundice, also affects this function, which we believe can be seen in the FS data.

For example, there is evidence in the literature of accumulation of vitamin A in hepatocytes with a decrease in serum levels in biliary cirrhosis and nonalcoholic fatty liver disease. This may indicate changes in retinol metabolism and distribution from the liver rather than a general deficiency.[66,67] Development of biliary cirrhosis may be a complication of bile duct obstruction.[68] There are also known results of a bile duct ligation experiment in rats, which showed a redistribution of vitamin A in the liver and its accumulation, while the level of retinol in the serum was decreased.[42] It was also noted that changes in vitamin A content have an effect on bile salt and acid homeostasis, which is also normally coregulated by vitamin A. It is possible that increased accumulation of vitamin A is necessary to prevent excessive liver damage in cholestasis. It is also worth noting that impaired bile outflow from the liver limits the levels of bile acids in the intestine, making it difficult to absorb vitamin A effectively.[42]

A key role in vitamin A metabolism is played by quiescent hepatic stellate cells, which store most of the vitamin A in the body in the form of retinyl esters.[69] Therefore, when serum retinol levels decrease, it is still unclear whether this indicates a general vitamin A deficiency or pathologic changes in its metabolism in the liver.[67] It is known that when the liver is damaged,

hepatic stellate cells are activated and transdifferentiate into proliferative myofibroblasts that produce collagens and fibronectins, leading to the development of fibrosis.[67] Fluorescence microscopy studies indicate that the spatial distribution of hepatic stellate cells overlaps with areas of fibrosis, resulting in parenchymal tissue collapse and decreased hepatocellular excretory function.[70] One of the factors that activates these cells is also aerobic glycolysis.[71] The fact that biliary obstruction causes cholestatic damage to the liver, including liver fibrosis, has been the subject of numerous reports.[68,72–75]

In this study, we also observed an increase in the contribution of fibrous proteins to the total fluorescence signal in the presence of obstructive jaundice. Although it did not reach statistical significance, this component may also be addressed in future studies. Thus, increased fluorescence of vitamin A may also be an indirect sign of decreased hepatocellular excretory function,[70] along with the accumulation of fibrous proteins as a predictor of the development of fibrosis. This parameter can also be used in the further development of a comprehensive parameter for the assessment of liver function in obstructive jaundice.

Based on the results obtained, we are considering continuing the analysis of the fluorescence spectra, taking into account the possible interrelated effects of vitamin A metabolism changes and the development of fibrosis, as well as the absorption of chromophores, especially hemoglobin,[56] which can greatly affect the recorded fluorescence spectra. For more accurate spectral deconvolution, it is also possible to pre-calibrate on pure solutions of selected fluorophores to obtain fluorescence spectra for the particular optical biopsy setup configuration used.

CONCLUSION

Currently, one of the urgent issues for surgeons in the treatment of obstructive jaundice is the ability to assess the functional state of the liver and to detect and determine the degree of liver failure in a timely manner. Since the liver has many functions in the human body, no single test can adequately assess all of them. A variety of laboratory and instrumental parameters are used to assess each liver function. In this regard, the use of optical techniques, which provide broad diagnostic capabilities in a wide range of biological and medical applications, seems promising. The use of FS method along with biochemical and imaging studies, including liver scintigraphy, elastography, ICG hepatic clearance, would allow one to more fully describe the functional state of the liver in obstructive jaundice. Incorporating new information on the metabolic status of the liver parenchyma into existing scales for assessing the severity of hepatocellular dysfunction will improve their diagnostic and prognostic efficacy.

In this work, we considered the feasibility of applying the method of FS to search for new diagnostic parameters of the functional state of the liver parenchyma in liver failure in the presence of obstructive jaundice. The results obtained reflect changes associated with shifts in the content of the main fluorophores characterizing hepatocyte dysfunction caused by accumulation of bilirubin and bile acids and after disturbance of oxygen utilization. The contributions of NAD(P)H, flavins, and bilirubin, as well as vitamin A, can be used for further studies as promising diagnostic and prognostic markers of the course of liver failure. While in this work and in future studies we propose an approach to assess the functional state of liver tissues by the FS method in post-hepatic jaundice, we also anticipate that in the long term it may be applicable to jaundice caused by another pre-hepatic and hepatic etiologies.

Further work will include collecting FS data in patients with different clinical effects of acute and prolonged obstructive jaundice on postoperative clinical outcome after biliary decompression. FS data will be compared with serum bilirubin levels, international normalized ratio, white blood cell count, and MELD score, which represent cholestasis, hemostasis, inflammation, and indirectly liver dysfunction, respectively. Another step is implementation of multimodal approach to optical biopsy. The results obtained will make it possible to further reduce the diameter of the fiber optic probe, which is critical for the study of parenchymal organs, and to apply the presented FS data processing both with other in vivo spectroscopy techniques (like diffuse reflectance spectroscopy) and in vitro methods for studying the properties of bile (namely, Raman spectroscopy).

LIMITATIONS

The needle probe approach to FS described in the article has some limitations. As a spectroscopic method, FS allows simultaneous measurement of only one point contacted by the fiber optic probe. To reduce measurement uncertainty, multiple measurements were taken at the surgeon's discretion. Since fluorescence spectra are recorded quickly (less than 1 min per point), one or two points were measured in the tissue along the path of the needle probe, depending on the patient's condition.

At this stage of the research, another limitation is the number of patients in the groups. The further development of new diagnostic criteria for the assessment of the functional state of the liver will require the collection of data from a larger sample of patients.

Finally, another serious limitation is the lack of a control group. Since surgery is performed because of pathology, it is obviously impossible to obtain in vivo data in healthy subjects.

ACKNOWLEDGMENTS

The research was supported by the Russian Science Foundation Grant No. 23-25-00487 (https://rscf.ru/en/project/23-25-00487/).

CONFLICT OF INTEREST STATEMENT

The authors declare no conflict of interest.

ORCID

Ksenia Y. Kandurova http://orcid.org/0000-0001-7940-3475
Andrian V. Mamoshin http://orcid.org/0000-0003-1787-5156
Elena V. Potapova http://orcid.org/0000-0002-9227-6308

REFERENCES

1. Hanif H, Khan SA, Muneer S, Adil SO. Diagnostic accuracy of ultrasound in evaluation of obstructive jaundice with MRCP as gold standard. Pak J Med Sci. 2020; 36(4): 652–6.
2. Duan F, Cui L, Bai Y, Li X, Yan J, Liu X. Comparison of efficacy and complications of endoscopic and percutaneous biliary drainage in malignant obstructive jaundice: a systematic review and meta-analysis. Cancer Imaging. 2017; 17(1): 1–7.
3. Pavlidis ET, Pavlidis TE. Pathophysiological consequences of obstructive jaundice and perioperative management. Hepatobiliary Pancreatic Dis Int. 2018; 17(1): 17–21.
4. Kong YL, Zhang HY, Liu CL, He XJ, Zhao G, Wang C, et al. Improving biliary stent patency for malignant obstructive jaundice using endobiliary radiofrequency ablation: experience in 150 patients. Surg Endosc. 2022; 36(3): 1789–98.
5. See TC. Acute biliary interventions. Clin Radiol. 2020; 75(5): 398.e9–398.e18.
6. Moole H, Bechtold M, Puli SR. Efficacy of preoperative biliary drainage in malignant obstructive jaundice: a meta-analysis and systematic review. World J Surg Oncol. 2016; 14(1): 1–11.
7. Shaib Y, Rahal MA, Rammal MO, Mailhac A, Tamim H. Preoperative biliary drainage for malignant biliary obstruction: results from a national database. J Hepatobiliary Pancreat Sci. 2017; 24(11): 637–42.
8. Galperin EI. Obstructive jaundice—a "false stable" condition, consequences of a "second hit", management principles. Annaly khirurgicheskoy gepatologii=Ann HPB Surg. 2011; 16(3): 16–25.
9. Lukmonov S. Minimally invasive biliary decompression methods in management of obstructive jaundice of malignant etiology. HPB. 2018; 20: S730.
10. Tanaka M, Tanaka K, Masaki Y, Miyazaki M, Kato M, Kotoh K, et al. Intrahepatic microcirculatory disorder, parenchymal hypoxia and NOX4 upregulation result in zonal differences in hepatocyte apoptosis following lipopolysaccharide-and D-galactosamine-induced acute liver failure in rats. Int J Mol Med. 2014; 33(2): 254–62.
11. Fedorov VE, Kharitonov BS, Masljakov VV, Logvina OE, Naryzhnaja MA. Features of mechanical jaundice course caused by complications of bile disease. Grekov's Bull Surg. 2020; 179(3): 48–57.
12. Rassam F, Olthof PB, Bennink RJ, van Gulik TM. Current modalities for the assessment of future remnant liver function. Visc Med. 2017; 33(6): 442–8.
13. Shahzad A, Knapp M, Edetsberger M, Puchinger M, Gaubitzer E, Köhler G. Diagnostic application of fluorescence spectroscopy in oncology field: hopes and challenges. Appl Spectrosc Rev. 2010; 45(1): 92–9.
14. Bratchenko IA, Sherendak VP, Myakinin OO, Artemyev DN, Moryatov AA, Borisova E, et al. In vivo hyperspectral imaging of skin malignant and benign tumors in visible spectrum. J Biomed Photonics Eng. 2018; 4(1): 5–12.
15. Kandurova K, Dremin V, Zherebtsov E, Potapova E, Alyanov A, Mamoshin A, et al. Fiber-optic system for intraoperative study of abdominal organs during minimally invasive surgical interventions. Appl Sci (Switzerland). 2019; 9(2): 217.
16. Zherebtsov E, Zajnulina M, Kandurova K, Potapova E, Dremin V, Mamoshin A, et al. Machine learning aided photonic diagnostic system for minimally invasive optically guided surgery in the hepatoduodenal area. Diagnostics. 2020; 10: 873.
17. Kim JA, Wales DJ, Yang GZ. Optical spectroscopy for in vivo medical diagnosis—a review of the state of the art and future perspectives. Prog Biomed Eng. 2020; 2(4): 42001.
18. Dunaev AV, Dremin VV, Zherebtsov EA, Rafailov IE, Litvinova KS, Palmer SG, et al. Individual variability analysis of fluorescence parameters measured in skin with different levels of nutritive blood flow. Med Eng Phys. 2015; 37(6): 574–83.
19. Palmer S, Litvinova K, Dunaev A, Fleming S, McGloin D, Nabi G. Changes in autofluorescence based organoid model of muscle-invasive urinary bladder cancer. Biomed Opt Express. 2016; 7(4): 1193–201.
20. Palmer S, Litvinova K, Dunaev A, Yubo J, McGloin D, Nabi G. Optical redox ratio and endogenous porphyrins in the detection of urinary bladder cancer: a patient biopsy analysis. J Biophotonics. 2017; 10(8): 1062–73.
21. Dremin V, Potapova E, Zherebtsov E, Kandurova K, Shupletsov V, Alekseyev A, et al. Optical percutaneous needle biopsy of the liver: a pilot animal and clinical study. Sci Rep. 2020; 10: 14200.
22. Voulgarelis S, Fathi F, Stucke AG, Daley KD, Kim J, Zimmerman MA, et al. Evaluation of visible diffuse reflectance spectroscopy in liver tissue: validation of tissue saturations using extracorporeal circulation. J Biomed Opt. 2021; 26(5): 55002.
23. Croce AC, Ferrigno A, Bertone V, Piccolini VM, Berardo C, Di Pasqua LG, et al. Fatty liver oxidative events monitored by autofluorescence optical diagnosis: comparison between subnormothermic machine perfusion and conventional cold storage preservation. Hepatol Res. 2017; 47(7): 668–82.
24. Palladini G, Di Pasqua LG, Cagna M, Croce AC, Perlini S, Mannucci B, et al. MCD diet rat model induces alterations in zinc and iron during NAFLD progression from steatosis to steatohepatitis. Int J Mol Sci. 2022; 23(12): 6817.
25. Zherebtsov EA, Potapova EV, Mamoshin AV, Shupletsov VV, Kandurova KY, Dremin VV, et al. Fluorescence lifetime needle optical biopsy discriminates hepatocellular carcinoma. Biomed Opt Express. 2022; 13(2): 633–46.
26. Keller A, Bialecki P, Wilhelm TJ, Vetter MK. Diffuse reflectance spectroscopy of human liver tumor specimens towards a tissue differentiating optical biopsy needle using light emitting diodes. Biomed Opt Express. 2018; 9(3): 1069–81.
27. Reistad N, Nilsson J, Timmermand OV, Sturesson C, Andersson-Engels S. Diffuse reflectance spectroscopy of liver tissue. In: Kurachi C, Svanberg K, Tromberg BJ, Bagnato VS, editors. Biophotonics South America. vol. 9531. SPIE; 2015. p. 587–96.
28. Croce AC, Ferrigno A, Bottiroli G, Vairetti M. Autofluorescence-based optical biopsy: an effective diagnostic tool in hepatology. Liver Int. 2018; 38(7): 1160–74.
29. Koenig K, Schneckenburger H. Laser-induced autofluorescence for medical diagnosis. J Fluoresc. 1994; 4(1): 17–40.
30. Croce AC, Ferrigno A, Santin G, Piccolini VM, Bottiroli G, Vairetti M. Autofluorescence of liver tissue and bile: organ functionality monitoring during ischemia and reoxygenation. Lasers Surg Med. 2014; 46(5): 412–21.

31. Poulon F, Pallud J, Varlet P, Zanello M, Chretien F, Dezamis E, et al. Real-time brain tumor imaging with endogenous fluorophores: a diagnosis proof-of-concept study on fresh human samples. Sci Rep. 2018; 8(1): 1–11.
32. Shrirao AB, Schloss RS, Fritz Z, Shrirao MV, Rosen R, Yarmush ML. Autofluorescence of blood and its application in biomedical and clinical research. Biotechnol Bioeng. 2021; 118(12): 4550–76.
33. Mathieu MC, Toullec A, Benoit C, Berry R, Validire P, Beaumel P, et al. Preclinical ex vivo evaluation of the diagnostic performance of a new device for in situ label-free fluorescence spectral analysis of breast masses. Eur Radiol. 2018; 28(6): 2507–15.
34. Braun F, Schalk R, Nachtmann M, Hien A, Frank R, Beuermann T, et al. A customized multispectral needle probe combined with a virtual photometric setup for in vivo detection of Lewis lung carcinoma in an animal model. Meas Sci Technol. 2019; 30(10): 104001.
35. Potapova E, Dremin V, Zherebtsov E, Mamoshin A, Dunaev A. Multimodal optical diagnostic in minimally invasive surgery. In: Tuchin VV, Popp J, Zakharov V, editors. Multimodal optical diagnostics of cancer. Cham: Springer; 2020. p. 397–424.
36. The International Commission on Non-Ionizing Radiation Protection. Guidelines on limits of exposure to ultraviolet radiation of wavelengths between 180 nm and 400 nm (incoherent optical radiation). Health Phys. 2004; 87(2): 171–86.
37. The International Commission on Non-Ionizing Radiation Protection. ICNIRP guidelines on limits of exposure to laser radiation of wavelengths between 180 nm and 1000 μm. Health Phys. 2013; 105(3): 271–95.
38. Datta R, Heaster TM, Sharick JT, Gillette AA, Skala MC. Fluorescence lifetime imaging microscopy: fundamentals and advances in instrumentation, analysis, and applications. J Biomed Opt. 2020; 25(7): 71203.
39. Bachmann L, Zezell DM, Ribeiro AdC, Gomes L, Ito AS. Fluorescence spectroscopy of biological tissues—a review. Appl Spectrosc Rev. 2006;41(6):575–90.
40. Mayevsky A, Chance B. Oxidation-reduction states of NADH in vivo: from animals to clinical use. Mitochondrion. 2007; 7(5): 330–39.
41. Schaefer PM, Kalinina S, Rueck A, von Arnim CAF, von Einem B. NADH autofluorescence—a marker on its way to boost bioenergetic research. Cytometry Part A. 2019; 95(1): 34–46.
42. Saeed A, Hoekstra M, Hoeke MO, Heegsma J, Faber KN. The interrelationship between bile acid and vitamin A homeostasis. Biochim Biophys Acta. 2017; 1862(5): 496–512.
43. Croce AC, Ferrigno A, Santin G, Vairetti M, Bottiroli G. Bilirubin: an autofluorescence bile biomarker for liver functionality monitoring. J Biophotonics. 2014; 7(10): 810–7.
44. Katz ML, Robison Jr. WG. What is lipofuscin? Defining characteristics and differentiation from other autofluorescent lysosomal storage bodies. Arch Gerontol Geriatr. 2002; 34(3): 169–84.
45. Sohal RS, Brunk UT. Lipofuscin as an indicator of oxidative stress and aging. Adv Exp Med Biol. 1989; 266: 17–26.
46. Croce AC, Bottiroli G. Autofluorescence spectroscopy and imaging: A tool for biomedical research and diagnosis. Eur J Histochem. 2014; 58(4): 320–37.
47. Croce AC, Ferrigno A, Di Pasqua LG, Berardo C, Mannucci B, Bottiroli G, et al. Fluorescing fatty acids in rat fatty liver models. J Biophotonics. 2017; 10(6–7): 905–10.
48. Croce AC, De Simone U, Freitas I, Boncompagni E, Neri D, Cillo U, et al. Human liver autofluorescence: an intrinsic tissue parameter discriminating normal and diseased conditions. Lasers Surg Med. 2010; 42(5): 371–78.
49. Chance B, Schoener B, Oshino R, Itshak F, Nakase Y. Oxidation-reduction ratio studies of mitochondria in freeze-trapped samples. NADH and flavoprotein fluorescence signals. J Biol Chem. 1979;254(11):4764–71.
50. Hu L, Wang N, Cardona E, Walsh AJ. Fluorescence intensity and lifetime redox ratios detect metabolic perturbations in T cells. Biomed Opt Express. 2020; 11(10): 5674–88.
51. Ramanujam N, Richards-Kortum R, Thomsen S, Mahadevan-Jansen A, Follen M, Chance B. Low-temperature fluorescence imaging of freeze-trapped human cervical tissues. Opt Express. 2001; 8(6): 335–43.
52. Alhallak K, Rebello LG, Muldoon TJ, Quinn KP, Rajaram N. Optical redox ratio identifies metastatic potential-dependent changes in breast cancer cell metabolism. Biomed Opt Express. 2016; 7(11): 4364–74.
53. Ciobanu DM, Olar LE, Stefan R, Veresiu IA, Bala CG, Mircea PA, et al. Fluorophores advanced glycation end products (AGEs)-to-NADH ratio is predictor for diabetic chronic kidney and cardiovascular disease. J Diabetes Complications. 2015; 29(7): 893–7.
54. Wang M, Long F, Tang F, Jing Y, Wang X, Yao L, et al. Autofluorescence imaging and spectroscopy of human lung cancer. Appl Sci. 2016; 7(1): 32.
55. Croce AC, De Simone U, Vairetti M, Ferrigno A, Bottiroli G. Autofluorescence properties of rat liver under hypermetabolic conditions. Photochem Photobiol Sci. 2007; 6(11): 1202–9.
56. Croce AC, Ferrigno A, Berardo C, Bottiroli G, Vairetti M, Di Pasqua LG. Spectrofluorometric analysis of autofluorescing components of crude serum from a rat liver model of ischemia and reperfusion. Molecules. 2020; 25(6): 1327.
57. Ercin CN, Bagci S, Yesilova Z, Aydin A, Sayal A, Erdem G. Oxidative stress in extrahepatic cholestasis. Anatol J Clin Investig. 2008; 2: 150–4.
58. Tiao MM, Lin TK, Wang PW, Chen JB, Liou CW. The role of mitochondria in cholestatic liver injury. Chang Gung Med J. 2009; 32(4): 346–53.
59. Okaya T, Nakagawa K, Kimura F, Shimizu H, Yoshidome H, Ohtsuka M, et al. Obstructive jaundice impedes hepatic microcirculation in mice. Hepato-gastroenterology. 2008; 55(88): 2146–50.
60. Blacker TS, Duchen MR. Investigating mitochondrial redox state using NADH and NADPH autofluorescence. Free Radical Biol Med. 2016; 100: 53–65.
61. Copple BL, Jaeschke H, Klaassen CD. Oxidative stress and the pathogenesis of cholestasis. Semin Liver Dis. 2010;30(2): 195–204.
62. Cichoż-Lach H, Michalak A. Oxidative stress as a crucial factor in liver diseases. World J Gastroenterol. 2014; 20(25): 8082.
63. Quinn KP, Sridharan GV, Hayden RS, Kaplan DL, Lee K, Georgakoudi I. Quantitative metabolic imaging using endogenous fluorescence to detect stem cell differentiation. Sci Rep. 2013; 3(1): 1–10.
64. Burkhardt M, Vollmar B, Menger MD. In vivo analysis of hepatic NADH fluorescence. In: Hudetz AG, Bruley DF, editors. Oxygen transport to tissue XX. Springer; 1998. p. 83–89.
65. Senoo H, Mezaki Y, Fujiwara M. The stellate cell system (vitamin A-storing cell system). Anat Sci Int. 2017; 92(4): 387–455.
66. Nyberg A, Berne B, Nordlinder H, Busch C, Eriksson U, Lööf L, et al. Impaired release of vitamin A from liver in primary biliary cirrhosis. Hepatology. 1988; 8(1): 136–41.
67. Saeed A, Bartuzi P, Heegsma J, Dekker D, Kloosterhuis N, de Bruin A, et al. Impaired hepatic vitamin A metabolism in NAFLD mice leading to vitamin A accumulation in hepatocytes. Cell Mol Gastroenterol Hepatol. 2021; 11(1): 309–25.
68. Geraghty JM, Goldin RD. Liver changes associated with cholecystitis. J Clin Pathol. 1994; 47(5): 457–60.
69. Schreiber R, Taschler U, Preiss-Landl K, Wongsiriroj N, Zimmermann R, Lass A. Retinyl ester hydrolases and their roles in vitamin A homeostasis. Biochim Biophys Acta. 2012; 1821(1): 113–23.

70. Vollmar B, Siegmund S, Menger MD. An intravital fluorescence microscopic study of hepatic microvascular and cellular derangements in developing cirrhosis in rats. Hepatology. 1998; 27(6): 1544–53.
71. Hou W, Syn WK. Role of metabolism in hepatic stellate cell activation and fibrogenesis. Front Cell Dev Biol. 2018; 6: 150.
72. MacMahon HE. A variant of obstructive biliary cirrhosis. Am J Pathol. 1970; 60(3): 371.
73. Aronson DC, Chamuleau RAFM, Frederiks WM, Gooszen HG, Heijmans HSA, James J. Reversibility of cholestatic changes following experimental common bile duct obstruction: fact or fantasy? J Hepatol. 1993; 18(1): 85–95.
74. Tag CG, Weiskirchen S, Hittatiya K, Tacke F, Tolba RH, Weiskirchen R. Induction of experimental obstructive cholestasis in mice. Lab Anim 2015; 49(Suppl 1): 70–80.
75. Kubo K, Kawakami H, Kuwatani M, Nishida M, Kawakubo K, Kawahata S, et al. Liver elasticity measurement before and after biliary drainage in patients with obstructive jaundice: a prospective cohort studya prospective cohort study. BMC Gastroenter. 2016; 16: 1–9.

How to cite this article: Kandurova KY, Sumin DS, Mamoshin AV, Potapova EV. Deconvolution of the fluorescence spectra measured through a needle probe to assess the functional state of the liver. Lasers Surg Med. 2023;1–12. https://doi.org/10.1002/lsm.23695